# New design of a detachable bulk-optic Faraday effect current clamp

**Benshun Yi**
**Beatrice C. B. Chu,** MEMBER SPIE
**Kin Seng Chiang,** MEMBER SPIE
City University of Hong Kong
Optoelectronics Research Centre
Department of Electronic Engineering
Tat Chee Avenue
Kowloon
Hong Kong
E-mail: eebcbchu@cityu.edu.hk

**Abstract.** We describe a new design of a detachable bulk-optic sensor for electric current detection. The sensor consists of two separate parts: an L-shaped arm cut to the critical angle and a straight arm to complement the L-shaped arm to form a right-angled triangular structure. With this design, the light beam needs to undergo only one total internal reflection along the optical path, making it more forgiving than the conventional design in terms of fabrication tolerance. An experimental sensor has been tested for its sensitivity to applied currents as well as to stray magnetic fields. *© 2001 Society of Photo-Optical Instrumentation Engineers.* [DOI: 10.1117/1.1365106]

Subject terms: Faraday effect; optical electric current sensor; bulk-optic sensor; magneto-optic sensor; current clamp.

Paper 200208 received May 29, 2000; revised manuscript received Dec. 29, 2000; accepted for publication Jan. 25, 2001.

## 1 Introduction

In the power industry, optical sensors are inherently advantageous over conventional measurement techniques.[1–4] Compared with conventional inductive type current transformers, optical current sensors (OCS) offer the advantages of being lightweight, small size, well insulated, large bandwidth, and immune to electromagnetic interference. An OCS can, in general, be defined as a device that consists of an optical sensing element that measures the line integral of the magnetic field along a closed optical loop around the current to be measured (the Faraday effect).[5] Many of the earlier proposed Faraday effect current sensors utilized optical fibers to provide the optical path around the conductor.[6,7] When an ordinary optical fiber is used, the sensitivity of the sensor is limited by the birefringence induced in the fiber. In the worst case, the Faraday effect can be quenched completely by the induced birefringence.[8] Furthermore, fiber-based OCSs are not detachable and, therefore, cannot be deployed or removed from the electrical wire without line disconnection. The use of bulk-optic glass for current sensing can overcome these problems.[9,10] In bulk form, materials with higher Verdet constants can be used and annealed to minimize the residual linear birefringence. In addition, a bulk-optic glass OCS can be readily designed into a detachable or clamp-on configuration that makes it attractive in temporary monitoring of load current without power line disconnection.[11]

To measure the Faraday effect with a bulk-optic glass sensor, it is necessary to guide the input light beam around the conductor in a closed loop. On any reflection surface, the light beam must undergo total internal reflection at the critical angle. A small deviation from the critical angle can change the polarization state of the light beam substantially and give rise to nonuniformity in sensitivity.[12,13] By using a triangular-shaped design, an OCS with reflection angles within a few seconds from the critical angle has been demonstrated.[14] However, the stringent requirements on the fabrication tolerance and optical alignment have limited the practicality of this type of sensor. To overcome the tolerance problem, a special design has been proposed, which is based on providing complementary effects on the polarization state[15,16] by using dual-quadrature reflections at each corner of a square-shaped sensor. Unfortunately, with this 3-D design, the optical path is no longer completely closed and the sensor is susceptible to the influence of stray magnetic fields.

We describe a new design for a detachable OCS. In this new design, the light beam undergoes only one total internal reflection along the optical path. This can relax substantially the fabrication tolerance and optical alignment. An experimental sensor has been tested and the results are reported.

## 2 Principle of Operation of the Sensor

Figure 1 shows the design of the sensor. The sensor is made of optical flint glass and comprised of two separate parts: a carefully cut L-shaped arm labeled sensing arm 1, and a straight arm labeled sensing arm 2, to close the opening of the L-shaped arm. These two parts form a right-angled triangular structure with a semicircular opening for passing through the current-carrying conductor. As shown in Fig. 1, the straight arm can be detached from the L-shaped arm to facilitate the placement of the current-carrying conductor. A polarizing beamsplitter (PBS) is placed at the base of the sensor to separate the input light beam into two orthogonal linearly polarized light beams, which are then launched into the two sensing arms, respectively. The light beam that propagates along the L-shaped arm needs to reflect once at the reflection corner. To preserve the state of polarization after reflection, the reflection corner is cut to an angle such that the beam is reflected at the critical angle. Since the sensor sensitivity depends strongly on the angle of reflection, a small deviation from the critical angle can severely affect the performance of the

 0091-3286/2001/$15.00 © 2001 Society of Photo-Optical Instrumentation Engineers

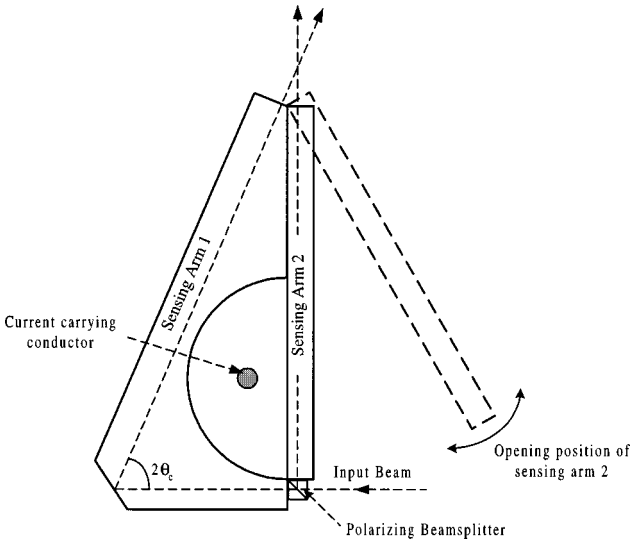


**Fig. 1** Design of the Faraday effect current clamp showing detachable sensing arms.

sensor.[13] In the previous design of a bulk-glass sensor based on critical angle reflection,[14] the light beam needs to be reflected at least twice within the sensor. Because the angles of incidence of the two reflections are interdependent, reflection corners of the glass must be polished to a high accuracy with an error less than a few seconds. This creates great difficulty in the manufacturing process and consequently increases the cost of the sensor. In this new design, however, the angle of incidence at the reflection corner can be controlled accurately by maneuvering the point of incidence of the light beam to the sensor. The tolerance on the reflection angle of the L-shaped arm can therefore be significantly relaxed. This feature can be considered as the major advantage of this design.

According to the Faraday effect, the polarization azimuth of a linearly polarized light beam propagating inside an optical element is rotated by an angle of $\Phi_F$ under the influence of a magnetic field $H$, generated by an electric current. Thus $\Phi_F$ is given by:

$$\Phi_F = V \int_l H dl, \tag{1}$$

where $l$ is the length of the optical element subject to the magnetic field and $V$ is the Verdet constant of the optical glass.

For our sensor shown in Fig. 2, after propagating along the respective sensing arms, the two beams together make up a closed optical loop. The magnetic field generated by the current $I_1$ in the internal conductor can rotate the polarization azimuths of the two light beams propagating inside sensing arms 1 and 2 by $\Phi_{11}$ and $\Phi_{21}$, respectively, with:

$$\Phi_{11} = V \int_{l_1} H_{11} dl_1 = \frac{\varphi_1}{2\pi} V I_1 \tag{2}$$

and

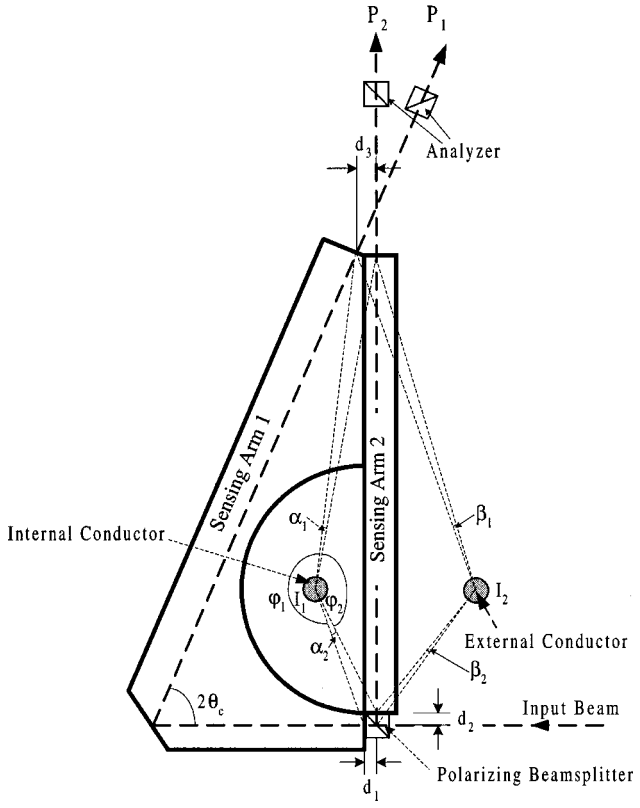


**Fig. 2** Schematic diagram of the sensor showing relevant parameters used in the analysis.

$$\Phi_{21} = V \int_{l_2} H_{21} dl_2 = \frac{\varphi_2}{2\pi} V I_1, \tag{3}$$

where $H_{11}$ and $H_{21}$ are the magnetic fields along the two sensing arms, respectively, $l_1$ and $l_2$ are the corresponding optical path lengths, and $\varphi_1$ and $\varphi_2$ are the angles subtended by the two arms, as shown in Fig. 2. Figure 3 illustrates the magnetic fields generated by the current $I_1$ and $I_2$ around the sensing arms, where the trajectory ''ABC'' represents the optical path along sensing arm 1, and the trajectory ''AC'' represents the optical path along sensing arm 2. It should be noted that the Faraday rotation angles $\Phi_{11}$ and $\Phi_{21}$ are complementary to each other. The sum of these two angles is equal to $VI_1$.

On the other hand, the Faraday rotation angles produced by the current $I_2$ in the external conductor are given by

$$\Phi_{12} = V \int_{l_1} H_{12} dl_1 \tag{4}$$

and

$$\Phi_{22} = V \int_{l_2} H_{22} dl_2 \tag{5}$$

for sensing arms 1 and 2, respectively, where $H_{12}$ and $H_{22}$ are the corresponding magnetic fields. The path $l_3$ shown in

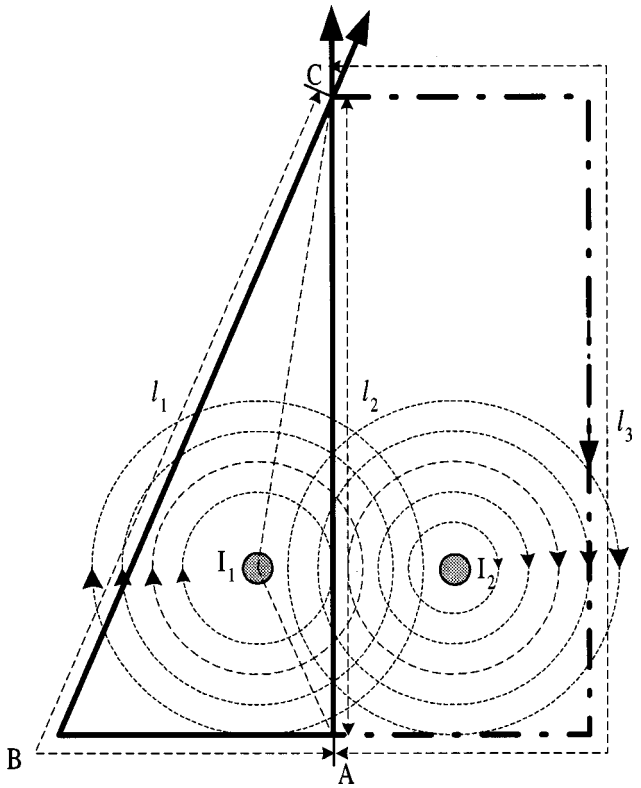


**Fig. 3** Optical paths for the calculation of the Faraday rotation angles produced by the currents $I_1$ and $I_2$.

Fig. 3 is a virtual common path shared by both sensing arms for the magnetic field generated by $I_2$. According to Ampere's circuital law, we have

$$\Phi_{12}=\Phi_{22}=VI_2-V\int_{l_3}H_{32}dl_3 \tag{6}$$

where $H_{32}$ is the magnetic field produced by $I_2$ along the path $l_3$.

After transversing along the two sensing arms, the two light beams pass through two analyzers that have their transmission axes set at 45 deg with respect to the polarization axes of the input light beams, respectively. As shown in Fig. 3, the magnetic fields generated by $I_1$ and $I_2$ add up in sensing arm 1 and cancel each other in sensing arm 2. The output signals from the analyzers $P_1$ and $P_2$ are given by

$$P_1=P_{01}\cos^2\left(\frac{\pi}{4}+\Phi_{11}+\Phi_{12}\right)$$

$$=\frac{P_{01}}{2}[1-\sin 2(\Phi_{11}+\Phi_{12})] \tag{7}$$

and

$$P_2=P_{02}\cos^2\left(\frac{\pi}{4}+\Phi_{22}-\Phi_{21}\right)$$

$$=\frac{P_{02}}{2}[1-\sin 2(\Phi_{22}-\Phi_{21})], \tag{8}$$

where $P_{01}$ and $P_{02}$ are the optical powers of the two beams. Two Faraday rotation signals $S_1$ and $S_2$ can be derived from $P_1$ and $P_2$ by using the conventional ac/dc signal recovery technique[1]:

$$S_1=\frac{P_1-P_{1dc}}{P_{1dc}}=\sin 2(\Phi_{11}+\Phi_{12}) \tag{9}$$

and

$$S_2=\frac{P_2-P_{2dc}}{P_{2dc}}=\sin 2(\Phi_{22}-\Phi_{21}), \tag{10}$$

where $P_{1dc}$ and $P_{2dc}$ are the dc components of the signals $P_1$ and $P_2$, respectively. Under the conditions $2(\Phi_{11}+\Phi_{12})\ll 1$ and $2(\Phi_{22}-\Phi_{21})\ll 1$, we can obtain the current $I_1$ by simply subtracting $S_2$ from $S_1$:

$$S=S_1-S_2\cong 2(\Phi_{11}+\Phi_{21})=2VI_1, \tag{11}$$

which gives a sensitivity of $2V$.

It can be seen from Fig. 3 that the internal field gives rise to Faraday rotation angles of opposite directions in the two sensing arms. This is because the light beams in the two sensing arms travel in opposite directions with respect to the direction of the magnetic field. On the other hand, the external field gives rise to identical Faraday rotation angles of the same direction in both sensing arms. This explains why in our design the signals from the two sensing arms, namely $S_1$ and $S_2$, must be subtracted from each other to cancel out the effects due to the external field. This principle differs markedly from that used in conventional closed loop designs where the internal field rotates the polarization angle of the light beam continuously in the same direction along the entire optical loop.

Equation (11) shows that the sensor is insensitive to any stray magnetic field. It should be pointed out that Eq. (11) is valid only under the ideal situation where the whole optical loop is inside the sensing glass and there exists negligible birefringence in the glass. In practice, however, a small part of the optical loop is inside the PBS and another part is exposed to air at the exit of the sensor, as shown by the paths $d_1$, $d_2$, and $d_3$ in Fig. 2. As a result, the sensitivity of the sensor may show some dependence on the position of the current-carrying conductor within the optical loop, as well as on the external field. With these imperfections taken into account, the total Faraday rotation angle becomes

$$\Phi\cong\left(1-\frac{\alpha_1+\alpha_2}{2\pi}\right)VI_1, \tag{12}$$

where $\alpha_1$ and $\alpha_2$ are the angles subtended by the paths in air and the PBS with respect to the internal conductor, re-

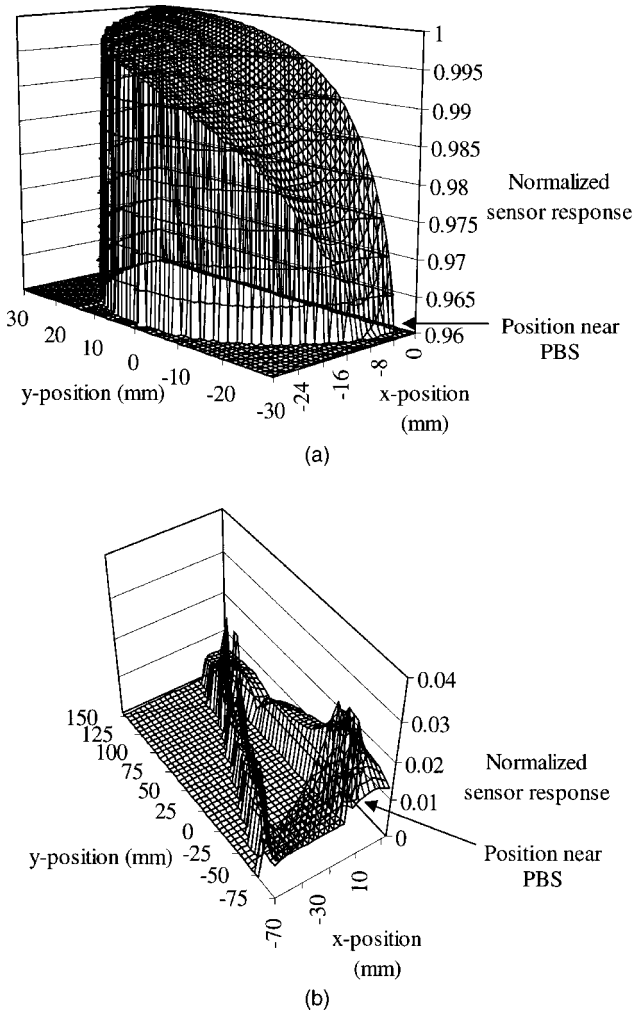


**Fig. 4** Computer simulation results showing (a) the sensitivity of the sensor as a function of the location of the conductor placed inside the semicircular hole of the sensor, and (b) the sensor response due to an external conductor placed at a distance within 30 mm around the sensor.

spectively, as shown in Fig. 2. We present in Fig. 4(a) the sensor response as a function of the location of the internal conductor (assuming zero diameter), taking $d_1 = d_3 = 2$ mm and $d_2 = 5$ mm (the values of the experimental set-up shown in Fig. 5). The origin of the *x-y* coordinate system in the computer simulation is set at the center of the semicircular opening of the L-shaped arm. It can be seen from Fig. 4(a) that the sensitivity of the sensor depends on the location of the current-carrying conductor. The sensitivity decreases gradually as the conductor is moved toward the PBS. The sensitivity can drop by ~3%. Normally, an accuracy of less than 5% is acceptable for fault monitoring and protection purposes in the power industry (the accuracy of most conventional current clamps is within this range). In practice, the worst sensitivity location can be avoided by shaping the opening of the L-shaped arm of the sensor in such a way that the conductor cannot be placed near the PBS.

The effect of an external field on the sensor response can be calculated by

$$\Delta\Phi_e \cong \frac{\beta_1 - \beta_2}{2\pi} V I_2, \tag{13}$$

where $\beta_1$ and $\beta_2$ are the angles subtended by the paths in air and the PBS with respect to the external conductor, respectively, as shown in Fig. 2. Here $\Delta\Phi_e$ is the error Faraday rotation signal induced by an external field. With the dimensions of the sensor shown in Fig. 5, the external conductor is assumed to be placed at positions within 30 mm from the sensor. The sensor response to the external field as a function of the location of the conductor is shown in Fig. 4(b). It can be seen from Fig. 4(b) that the nearer the external conductor is placed to the PBS or to the exits of the sensing arms, the more severe is the effect. In the worst case, where the external conductor is closest to the PBS, an error of 3.5% can be introduced.

## 3 Experiments and Results

The experimental set-up of the sensor is shown schematically in Fig. 5. Both the L-shaped arm (125×52 mm) and the straight arm (106×12 mm) of the sensor were made of SF-6 flint glass, which had been annealed to eliminate intrinsic birefringence. The radius of the semicircular opening was 30 mm. According to the glass supplier, the angle at the reflection corner was polished to the critical angle, 33°44′42″, with an error less than fifteen seconds. It should be emphasized, however, that such a high precision in the cutting angle was unnecessary. A light beam from a 2 mW He-Ne laser, at 632.8 nm, was launched into a PBS. The PBS separated the input light into two orthogonal linearly polarized beams, which were then launched into the two sensing arms of the sensor, respectively. The He-Ne laser was mounted on a rotatable translation stage so that both the angle of incidence and the entry point of the light beam could be adjusted precisely. To ensure that the light beam was reflected at the critical angle at the corner of the L-shaped arm, the position of the laser was adjusted continuously until the light beam refracted from the corner just vanished. Care was taken to avoid the angle of incidence from going below or beyond the critical angle, since reflection at an angle other than the critical angle can result in an alteration of the incident polarization state, and thus affect the sensitivity of the sensor severely.[13]

After traveling through the respective sensing arms, the two beams passed through two analyzers that had their polarization axes set at 45 deg with respect to the axes of the PBS. The output beams from the analyzers were detected and processed by two identical signal processing units, which consisted of a PIN photodiode, a transimpedance amplifier (A), a low-pass filter (LPF), and a subtractor. The signal processing unit separated the signal into its ac and dc components, which were then recorded by two FLUKE digital multimeters (DMM). The signals $S_1$ and $S_2$, as given in Eqs. (9) and (10), respectively, were calculated by dividing the ac component over the dc component of the respective output signals. The signal $S$ was calculated in accordance with Eq. (11). As the signals $S_1$ and $S_2$ were detected by two separate signal processing units, any variation in the light intensities due to the polarization dependence of the PBS did not affect the result. The ac/dc method employed in our sensor gives the same sensitivity

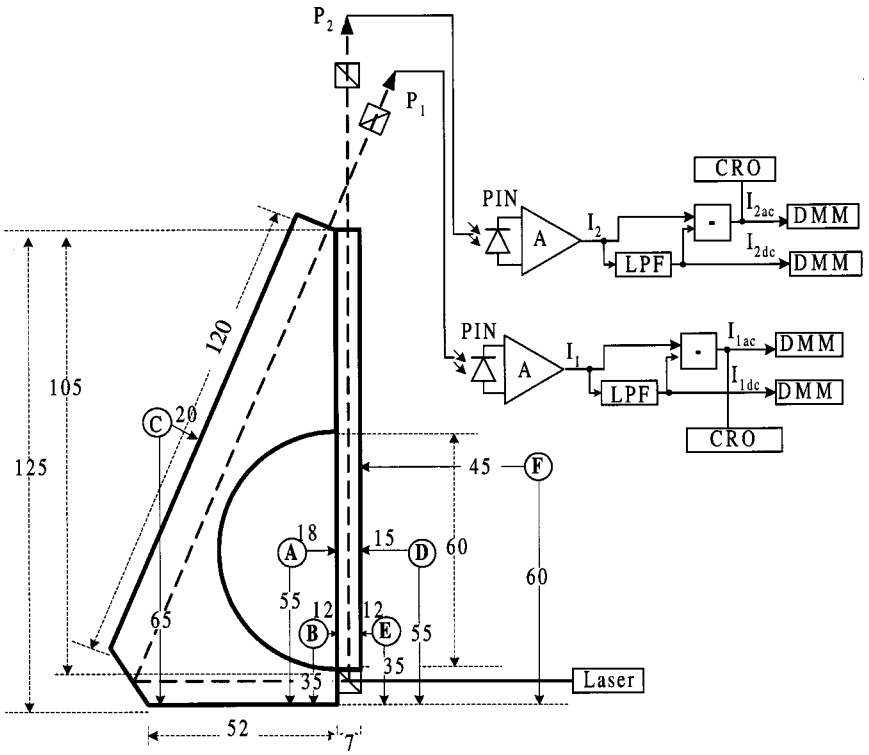


**Fig. 5** Experimental set-up of the Faraday effect current sensor. The distances indicated in the diagram are measured in millimeter.

as the difference-over-sum method, which is also a common method in retrieving the Faraday rotation signal. Although the latter method can give improved rejection to common-mode noise in the signal, e.g., fluctuations in the light intensity, its optical hardware is more complex and expensive.[2]

When the sensor is operated as a current clamp, the straight arm of the sensor can be removed and refitted to the L-shaped arm as illustrated in Fig. 1. The straight arm should be in good contact with the L-shaped arm. According to our calculation, a separation of 1 mm between the sensing arms near the PBS results in a decrease of sensitivity by ~1%, which compares favorably with a previous design,[11] where an air gap of less than 0.33 mm between two sensing parts must be maintained for the same performance. The relatively low tolerance in the previous design is due to the fact that an air gap can upset the critical angle reflection. In our present design, however, the opening mechanism does not affect the angle of reflection in the L-shaped arm, and hence, the tolerance can be much relaxed.

As already mentioned, the optical paths made up by the two beams do not form a perfectly closed optical loop. As a result, the sensor response depends on both the locations of the internal current and the external field. A series of experiments were performed to measure the significance of such dependence and confirm the sensor sensitivity. In the experiments, two positions of placing the internal current and four positions of placing the external current were tested, as indicated by positions A, B, C, D, E, and F in Fig. 5.

In the first experiment, a 20-mm-diam conductor, which carried 1000A current, was placed at position A within the optical loop. The sensor response to the 50-Hz applied current was measured and the results obtained are presented in Fig. 6. As shown in Fig. 6, the signal varied linearly with the applied current. The sensitivity was measured to be $(4.45 \pm 0.06) \times 10^{-5}$ rad/A, which agrees well with the calculated value $2V = 4.46 \times 10^{-5}$ rad/A, given that the Verdet constant for SF-6 glass is $2.23 \times 10^{-5}$ rad/A.[17]

We next placed the conductor at different positions, as indicated in Fig. 5. For each position, a fixed current of 1000A was applied to the conductor and the sensor sensi-

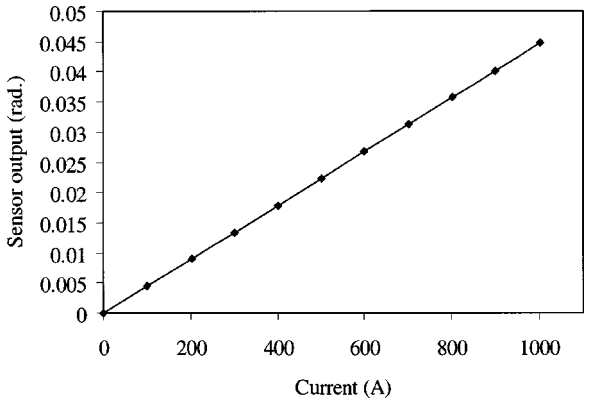


**Fig. 6** Sensor output as a function of applied current placed at position A within the optical loop (Fig. 5).

**Table 1** Current sensitivities measured by placing a 1000A current-carrying conductor at positions A, B, C, D, E, and F, as indicated in Fig. 5.

| Position of conductor | Current sensitivity ($\times 10^{-5}$ rad/A) | Error to the measurement of the internal current | Calculated errors |
|---|---|---|---|
| A | 4.45 | 0.2% | 0.5% |
| B | 4.41 | 1.1% | 0.8% |
| C | 0.05 | 1.1% | 1.1% |
| D | 0.06 | 1.3% | 1.2% |
| E | 0.07 | 1.6% | 1.5% |
| F | 0.02 | 0.5% | 0.5% |

tivity was measured. To eliminate fluctuations due to the instability of the current source, a number of measurements were taken for each position over a time period of five minutes. The average values of the measurements and the calculated values are tabulated in Table 1.

As shown in Table 1, the current sensitivities measured at positions A and B are $4.45\times10^{-5}$ rad/A and $4.41\times10^{-5}$ rad/A, respectively, which deviate from the value of $2V$ by 0.2% and 1.1%, respectively. As expected, the sensitivity drops at position B near the PBS. The experimental results agree reasonably well with the calculated values 0.5% (position A) and 0.8% (position B), which take into account the finite size of the conductor. As mentioned before, the semicircular opening of the L-shaped sensing arm can be reshaped to avoid the internal conductor being placed too close to the PBS. It should be possible to achieve a sensitivity uniformity better than 1%.

The sensitivities measured at positions C, D, E, and F are $0.05\times10^{-5}$ rad/A, $0.06\times10^{-5}$ rad/A, $0.07\times10^{-5}$ rad/A, and $0.02\times10^{-5}$ rad/A, respectively. The corresponding contributions to the sensitivity of measuring the internal current are 1.1%, 1.3%, 1.6%, and 0.5%, which again agree well with the calculated values. As expected, the largest response due to the external field was obtained at position E, which was closest to the PBS, whereas the weakest response was obtained at position F, which was farthest from the sensor. In practice, an external conductor is seldom located next to the sensor, and the influence from the external field can be kept at a negligible level.

## 4 Conclusion

A novel design of a detachable Faraday effect current sensor has been described. The sensor consists of two separate Faraday rotation sensing arms for guiding two separate light beams to form an approximately closed optical loop. With this new arrangement, the fabrication tolerance on the sensor can be relaxed significantly. We have built and tested an experimental sensor to confirm the expected performance of the design. In particular, we have studied the sensitivity uniformity of the sensor and its response to external stray magnetic fields. In both aspects, the sensor performs well. We believe that the sensor could be further developed into a practical device with application in the power industry.

### Acknowledgments

This research was supported by a research grant from the Research Grant Council of the Hong Kong Special Administration Region, China (project no. CityU 1044/97E).

### References

1. M. Kanoi, G. Takahashi, T. Sato, M. Higaki, E. Mori, and K. Okumura, ''Optical voltage and current measuring system for electric power systems,'' *IEEE Trans. Power Deliv.* **1**(1), 91–97 (1986).
2. IEEE Power Systems Instrumentation and Measurement Committee, ''Optical current transducer for power system: a review,'' *IEEE Trans. Power Deliv.* **9**(4), 1778–1787 (1994).
3. Y. N. Ning, Z. P. Wang, A. W. Palmer, K. T. V. Grattan, and D. A. Jackson, ''Recent progress in optical current sensing techniques,'' *Rev. Sci. Instrum.* **66**(5), 3097–3111 (1995).
4. T. Bosselmann, ''Magneto- and electro-optic transformers meet expectation of power industry,'' *Proc. OFS'97*, pp. 111–114, Williamsburg, Virginia (1997).
5. G. W. Day and A. H. Rose, ''Faraday effect sensors, the state of art,'' *Proc. SPIE* **985**, 138–151 (1988).
6. A. Rapp and H. Harms, ''Magnetooptical current transformer,'' *Appl. Opt.* **19**(22), 3729–3745 (1982).
7. A. M. Smith, ''Optical fibers for current measurement applications,'' *Opt. Laser Technol.* **12**(1), 25–29 (1980).
8. P. R. Former and F. C. Jahoda, ''Linear birefringence effects on fiber optics current sensors,'' *Appl. Opt.* **27**(15), 3088–3096 (1988).
9. Y. N. Ning, B. C. B. Chu, and D. A. Jackson, ''Miniature Faraday current sensor based on multiple critical angle reflections in a bulk-optic ring,'' *Opt. Lett.* **16**(24), 1996–1998 (1991).
10. B. Yi, B. C. B. Chu, K. S. Chiang, and H. S. H. Chung, ''New design of optical electric-current sensor for sensitivity improvement,'' *IEEE Trans. Instrum. Meas.* **49**(2), 418–423 (April 2000).
11. Y. Ning and D. A. Jackson, ''Faraday effect optic current clamp using a bulk glass sensing element,'' *Opt. Lett.* **18**, 835–837 (1993).
12. S. P. Bush and D. A. Jackson, ''Numerical investigation of the effects of birefringence and total internal reflection on Faraday effect current sensors,'' *Appl. Opt.* **31**(25), 5366–5374 (1992).
13. B. C. B. Chu, Y. N. Ning, and D. A. Jackson, ''Polarization analysis of bulk optic Faraday current sensor with a triangular configuration,'' *Proc. SPIE* **1746**, 128–138 (1992).
14. B. C. B. Chu, Y. N. Ning, and D. A. Jackson, ''A Faraday current sensor using a triangular-shaped bulk optic sensing element,'' *Opt. Lett.* **17**(16), 1167–1169 (1992).
15. T. Sato, G. Takahashi, and Y. Inui, Europe Patent, Publication no. 0088419A1 (1983).
16. A. H. Rose, M. N. Deeter, and G. W. Day, ''Submicroamphere-per-root-hertz current sensor based on the Faraday effect in Ga:YIG,'' *Opt. Lett.* **18**(17), 1471–1473 (1993).
17. Optical glass data sheets from SCHOTT Optical Glass, Inc., Germany (1998).

**Benshun Yi** received the BEng, MEng, and PhD degrees in electrical engineering from Huazhong University of Science and Technology, Wuhan, China, in 1986, 1989 and 1996, respectively. From 1996 to 1997, he spent one year as a visiting scholar in the Centre for Electrical Power Engineering at Strathclyde University, Glasgow, United Kingdom. In September 1998, he joined the Optoelectronics Research Centre, Department of Electronic Engineering, City Uni-

versity of Hong Kong where he is currently a senior research associate. His current research interests include optical sensors for power industry, fibre Bragg grating sensors and precision instrumentation.

**Beatrice C. B. Chu** received her BSc and PhD degrees in physics from the University of Kent at Canterbury, United Kingdom, in 1988 and 1992, respectively. In 1993, she was appointed as visiting research associate at the Applied Optics group at the University of Kent. In March 1994, Dr. Chu was appointed as visiting fellow for a period of six months at the City University of Hong Kong, Since September 1994, Dr. Chu is appointed assistant professor at the Department of Electronic Engineering at the City University of Hong Kong. Dr. Chu's main research area is in the area of optical sensing techniques, especially in the utilization of the Faraday effect for electric current measurement with different topologies, using both the optical fibre and bulk-optics glass as the sensor elements. Dr. Chu is a member of the Optical Society of America, the International Society for Optical Engineering (SPIE), and the Institute of Electrical and Electronic Engineering.

**Kin Seng Chiang** received the BE (Hon. I) and PhD degrees in electrical engineering from the University of New South Wales, Sydney, Australia, in 1982 and 1986, respectively. In 1986, he spent six months in the Department of Mathematics at the Australian Defense Force Academy, Canberra. From 1986 to 1993, he was with the Division of Applied Physics of the Commonwealth Scientific and Industrial Organization (CSIRO), Sydney. From 1987 to 1988, he received a Japanese government research award and spent six months at the Electrotechnical Laboratory, Tsukuba City, Japan. From 1992 to 1993, he worked concurrently for the Optical Fibre Technology Centre (OFTC) of the University of Sydney. In August 1993, he joined the City University of Hong Kong, where he is currently a chair professor. He has published over 180 papers on optical waveguide/fiber theory and characterization, numerical methods, fiber devices and sensors, and nonlinear guided-wave optics. Dr. Chiang is a member of the Optical Society of America, the International Society for Optical Engineering (SPIE), and the Australian Optical Society.